Control of NMR-laser chaos in high-dimensional embedding space

C. Reyl and L. Flepp
Physik-Institut der Universität, Schönberggasse 9, 8001 Zurich, Switzerland

R. Badii
Paul Scherrer Institute, 5232 Villigen, Switzerland

E. Brun
Physik-Institut der Universität, Schönberggasse 9, 8001 Zurich, Switzerland
(Received 17 July 1992)

The unstable periodic orbits of a chaotic NMR laser have been identified and classified according to their stability properties. The dynamical control method by Ott, Grebogi, and Yorke (OGY) [Phys. Rev. Lett. **64**, 1196 (1990)] has been successfully applied in a six-dimensional embedding space, as required for a proper reconstruction of the attractors. An improved method has then been implemented in order to circumvent the occurrence of several, possibly complex, unstable eigenvalues in the standard OGY procedure and has shown superior performance. Finally, an extension to several control stations per Poincaré time is discussed.

PACS number(s): 05.45.+b, 76.60.−k

INTRODUCTION

Chaotic behavior is a commonly observed phenomenon in a large number of physical systems such as hydrodynamical flows, nonlinear-optical devices, mechanical or electronic oscillators, and nuclear magnetic resonators. The dynamics in phase space is deeply influenced by the existence of an infinity of unstable periodic orbits. The aperiodic trajectory describing the system's evolution is attracted to any one of these when it approaches the stable manifold and is repelled to some other region when it finds itself in the vicinity of the unstable one. Because of its invariance under smooth coordinate changes, the set of unstable periodic orbits provides a topological characterization of the dynamics which facilitates the construction of a faithful mathematical model from the observation of even a single scalar time series [1]. The study of the periodic-orbit structure can be profitably extended to the evaluation of dynamical (metric) invariants, such as the Lyapunov exponents, related to the attractive and repulsive properties of the orbits. This knowledge can be used to perform finite-time predictions about the system evolution [2], to reduce the effect of noise on the measured data [3], or even to constrain the motion to the close neighborhood of some unstable periodic orbit. The latter practice is called control and is usually carried out by applying small, carefully chosen, perturbations to a control parameter. The method, originally proposed by Ott, Grebogi, and Yorke (OGY) [4], requires that the displaced trajectory lie as close as possible to the stable manifold of the target orbit γ. In a practical implementation, after having located the selected orbit in a suitable embedding space, it is necessary to approximate the flow around it by means of a matrix $\mathbf{M}$ (usually estimated through a least-squares fit). It is further assumed that the target orbit is of the saddle type, so that its invariant manifolds can be identified with the eigendirections of the matrix $\mathbf{M}$ in an ϵ ball centered at some reference point $\mathbf{x}_F$ on γ. The dependence of the motion on a control parameter p is simply evaluated by comparing $\gamma(p=0)$ with the perturbed orbit $\gamma(p)$ which is also to be extracted from the observed data. For the case in which only one unstable direction exists, the required correction is given by the simple expression [4]

$$p=\lambda_u(\lambda_u-1)^{-1}[(\xi-\xi_F)\cdot\mathbf{f}_u]/(\mathbf{g}\cdot\mathbf{f}_u)\ , \tag{1}$$

where the curve γ has been cut by a Poincaré section Ξ through $\mathbf{x}_F$ (yielding the point ξ_F). The value p hence depends on the current position ξ on Ξ, on the unstable eigenvalue λ_u of $\mathbf{M}$, and on the projection of the difference vector $\xi-\xi_F$ along the the contravariant basis vector $\mathbf{f}_u$. The overall magnitude is finally weighted by the term $\mathbf{g}\cdot\mathbf{f}_u$, where $\mathbf{g}=\partial\xi_F(p)/\partial p|_{p=0}$ expresses the sensitivity of the system to perturbations. Notice that the Poincaré section Ξ has only been introduced to simplify the presentation and is not, in fact, essential.

This method presents a few distinctive features: the knowledge of the underlying exact equations is not needed, although effective use of the linearized dynamics in embedding space is made; the target orbit can be explicitly chosen and the computations involved are relatively simple. However, expression (1) becomes inappropriate as soon as several unstable or complex eigenvalues occur. An extension to the higher-dimensional case is nevertheless possible (as shown in [5]) although the procedure becomes rather cumbersome. The major source of inaccuracy comes from the evaluation of the eigenvalues with the corresponding contravariant vectors and of the "flow derivative" $\mathbf{g}$: in fact, they fluctuate considerably from run to run, so that the control is not frequently reproducible in certain regions of parameter space.

Therefore, while retaining the positive characteristics

of the method, we implemented an alternative technique which is affected neither by the occurrence of more than one unstable direction nor by the possible complexity of the eigenvalues. The control condition which substitutes Eq. (1) is obtained by requiring that the expected deviation of the orbit from the target be minimized by our choice of p (minimal expected deviation method or MED). Our prediction is based on the same matrix $\mathbf{M}$ as for the OGY procedure, although the dynamics may now be approximated by a more general nonlinear map as well. No estimate of the eigenvalues and of the corresponding contravariant vectors is needed, thus yielding higher reproducibility of the control. The vector $\mathbf{g}$ is, however, still determined as before. Finally, the method may easily be implemented with several control stations along the target orbit.

The OGY procedure has so far been implemented in Ref. [6], where a driven magnetoelastic ribbon has been controlled around the periodic orbits of order 1 and 2. Since the two-dimensional Poincaré map was always single valued in the neighborhood of these orbits, the procedure was considerably simplified. Moreover, the forcing frequency $\nu=0.85$ Hz was rather low, so that plenty of time was available to perform the numerical calculations and send the control signal to the system. We applied both the OGY and the MED methods to a NMR laser which displays attractors with dimension in the range (2.2,2.6), upon modulation of a parameter with a frequency ν of the order of 100–120 Hz. Although the minimal embedding dimension is, in this case, $E=5-6$ and the operating frequency about 120 times higher than that of Ref. [6], control has been achieved under several conditions for the lowest periodic orbits.

Notice that generic reductions of chaotic motion to periodic behavior have been made recently by various groups. Some of these methods consist of a simple feedback or modulation mechanism which does not require any calculation [7–10]. Although valuable for their simplicity and achievable speed, these techniques allow one to predict neither the type of periodic orbit which is induced by the perturbation nor the amplitude of the latter. They rely to a considerable extent on empirical criteria and cannot be really regarded as controlling processes but rather as stabilization methods. On the other hand, periodic entrainment of chaotic motion has been obtained by forcing the system to follow the behavior of model equations for the target dynamics [11]: the amplitude of the perturbations depends on the distance between the chaotic attractor and the aimed orbit and need not be small.

I. IDENTIFICATION OF PERIODIC ORBITS

We applied the control techniques to a parametrically modulated NMR laser. The system [12] consists of a ruby crystal placed at a temperature of 4.2 K in a static magnetic field $\mathbf{B}_0$ of magnitude 1.1 T. The laser activity is provided by the nuclear spins of the ^{27}Al in the crystal. The population inversion is obtained by means of a microwave pump and the resonance by enclosing the spins in a cavity which consists, in our case, of an LC circuit providing the feedback radiation field $\mathbf{B}$, necessary for coherent spin-flip behavior. The circuit quality factor Q is furthermore sinusoidally modulated as $Q(t)=Q_0(1+A\cos\omega t)$, where $\omega/2\pi\in(100,120)$ Hz. The NMR laser exhibits chaotic behavior in a wide range of parameter values (Q_0, A and ω), characterized by low-noise output and absence of noticeable drift. The data have been recorded with a 12-bit-resolution analog-to-digital translation board by sampling the output voltage [proportional to the nuclear transverse magnetization $M_t(t)$] at a frequency $\nu=24/T\in(2400,3000)$ Hz, where $T=2\pi/\omega$ is the period of the forcing term. Time series of length $N=1.5\times10^5$ were usually stored for subsequent analysis. The data $z_i=M_t(i/\nu)$ have been embedded in an E-dimensional space X. Its points are given in the form $\mathbf{x}_k=\{z_k,z_{k-\tau},\ldots,z_{k-\tau(E-1)}\}$, where $\tau=4$ and τ/ν is the appropriate delay time.

The information dimension D of the chaotic NMR-laser attractor lies in the interval (2.2,2.6), depending on the parameter values [13]: hence the minimal embedding dimension required for a proper reconstruction of the attractor is $E=6\geq 2D+1$ [14]. The embedding window τE spans a whole period of the forcing term. Unstable periodic orbits of order up to 6 (i.e., of period $6T$) have been located by the method of close returns [1] simultaneously with the acquisition of data points. The existence of a return in a region $B_{\epsilon_{i_0}}$ of size ϵ_{i_0} around point $\mathbf{x}_{i_0}$ is tested by following the trajectory $\{\mathbf{x}_i\}$ for all $i\in[i_0+t_{\min},i_0+t_{\max}]$, until the condition $d(\mathbf{x}_i,\mathbf{x}_{i_0})\equiv\|\mathbf{x}_i-\mathbf{x}_{i_0}\|\leq\epsilon_{i_0}$ is satisfied for some index i. A return consists then of a pair $(\mathbf{x}_i,\mathbf{x}_{i+n})$, with n close to a multiple of νT, which satisfies the above inequality. The (integer) times $t_{\min}$ and $t_{\max}$ help in selecting the lengths of the orbits to be investigated. The precision ϵ_{i_0} has been chosen proportional to the norm of the local velocity in phase space:

$$\epsilon_{i_0}^2=a\frac{1}{\tau}\sum_{k=k_0+1}^{k_0+\tau}\|\mathbf{x}_k-\mathbf{x}_{k-1}\|^2,\quad k_0=i_0-[\tau/2]\,, \tag{2}$$

where $a\in(0.3,0.6)$ is a user-specified constant, $\tau=4$ is the discrete delay time, and [ ] denotes the integer part. This choice yields higher resolution in portions of phase space where the data points are very close to each other. A return $(\mathbf{x}_i,\mathbf{x}_{i+n})$ can be refined by computing $d_{i+1}\equiv d(\mathbf{x}_{i+1},\mathbf{x}_{i+n+1})$ and checking whether the relative distance d_{i+1}/ϵ_{i+1} has decreased or not with respect to d_i/ϵ_i. If this is the case, the procedure is repeated until an increase is found, thus determining the best return. In order to avoid collapse of the distances below the noise level, we introduce a cutoff proportional to $b\sqrt{E}$, where $b=2^{-12}$ is the sample resolution.

II. FITTING THE RETURN MAP AND ESTIMATING THE STABILITY PROPERTIES

Once an unstable orbit γ of period T_γ has been identified, the dynamics around it can be approximated

by means of one or more (linear) maps. Following [4], we introduce a surface of section $\Xi \in X$ in order to reduce the dimensionality of the problem and to simplify the exposition (this step is not strictly necessary, in fact). Indicating with $\mathbf{x}_F \equiv (x_F^{(1)}, \ldots, x_F^{(E)})$ the control "station" on γ, the section is defined as $\Xi \equiv \{\mathbf{x}: x^{(1)} = x_F^{(1)}\}$, where $\mathbf{x} \equiv (x^{(1)}, \ldots, x^{(E)})$. This choice always yielded a plane transversal to the vector flow in the neighborhood $B_\epsilon(\mathbf{x}_F)$ of $\mathbf{x}_F$. For each portion of trajectory passing through $B_\epsilon(\mathbf{x}_F)$ both at times t and $t + T_\gamma$, we choose the closest return $(\mathbf{x}_i, \mathbf{x}_{i+n})$ (where $n \approx \nu T_\gamma$) and associate to $\mathbf{x}_i$ an intersection point ξ_i on Ξ, determined by linear interpolation (between the first two images or preimages of $\mathbf{x}_i$ which lie on opposite sides of Ξ). Since, by definition, $\mathbf{x}_F \in \Xi$, we shall indicate it with ξ_F in the following, for homogeneity of notation. The requirement that both start and end points of the returning trajectory belong to $B_\epsilon(\mathbf{x}_F)$ guarantees that the target orbit γ is shadowed for a time length $T_\gamma + T$, since the embedding window (which has been taken backwards in time) spans a period T.

Assuming, as a first approximation, that the dynamics from $B_\epsilon(\xi_F)$ to itself is linear, we can write

$$\xi_{n+1} - \xi_F \simeq \mathbf{M}[\xi_n - \xi_F] , \tag{3}$$

where $\mathbf{M} = \mathbf{D}_\xi \mathbf{F}(\xi_F)$ is the Jacobian matrix of the (reduced) Poincaré map $\mathbf{F}$: $B_\epsilon(\xi_F) \to B_\epsilon(\xi_F)$. The matrix $\mathbf{M}$ has been estimated with a least-squares procedure which makes use of singular-value decomposition [15], using a collection of m ($m = 50$–100) vector pairs $(\delta\xi, \delta\xi')$ in $B_\epsilon(\xi_F)$, where $\delta\xi = \xi - \xi_F$ and $\delta\xi' = \mathbf{F}(\delta\xi)$.

A simple noise-reduction method can be implemented to enhance the quality of the fit by discarding the vector pairs for which a considerable discrepancy is found between actual and predicted image of the starting point: i.e., point ξ_i is neglected if

$$\|\delta\xi' - \mathbf{M}\delta\xi\| > \epsilon_{\max} , \tag{4}$$

where $\mathbf{M}\delta\xi$ and $\delta\xi'$ are the expected and observed vectors, respectively, and $\epsilon_{\max}$ is a suitable cutoff. A new matrix $\mathbf{M}$ is then estimated from the "cleaned" set of points in Ξ. This step can be further iterated. Notice that a barrel-shaped neighborhood is obtained, since the rejected points lie at the border of the ball, close to the unstable manifold. The same procedure can be adopted with minor modifications to handle the case of $L > 1$ control stations along the target orbit γ. This has been implemented with $L = 2$ to 4, obtaining considerably better predictions of the dynamics. Then, one has L matrices $\mathbf{M}_l$: $B_\epsilon(\mathbf{x}_l) \to B_\epsilon(\mathbf{x}_{l+1})$, with $l = 1, \ldots, L$ and $\mathbf{x}_{L+1} = \mathbf{x}_1$.

The stability properties of γ are determined by the eigenvalues of $\mathbf{M}$ which are computed by balancing the matrix in order to reduce its overall norm, by transforming it to Hessenberg form and, finally, by applying the standard QR algorithm [15]. The corresponding eigenvectors are evaluated by inverse iteration. The case of complex eigenvalues requires more sophisticated methods including, of course, computation in complex arithmetic. We found complex eigenvalues many times, especially for orbits of period 3 or higher and when there were several control stations per orbit. This fact shows rotation of the vector flow. The occurrence of complex eigenvalues requires modification of the standard OGY method. Moreover, when several unstable directions are present, a generalization of that control algorithm is needed [5]. Both issues severely restrict the range of applicability of OGY's method. Notice that application to the NMR laser is further complicated by the speed of the system: the dynamics is, in fact, about 120 times quicker than for the magnetoelastic ribbon of Ref. [6] (and must be reconstructed in a higher-dimensional space). Therefore we developed an alternative control algorithm.

III. MINIMAL EXPECTED DEVIATION METHOD

In order to circumvent the above-mentioned problems, we developed a method which relies on predictions of the local dynamics and employs a different control condition than OGY's. While the extraction and identification of the unstable periodic orbits and the fitting of the return map take place exactly as before, it is no longer necessary to compute the stability properties of the chosen orbit. Rather than demanding that the perturbed point $\xi_{n+1}(p)$ falls onto the stable manifold of the target orbit [i.e., $\mathbf{f}_u \cdot \xi_{n+1}(p) = 0$, yielding Eq. (1)], we require that it comes as close as possible to the control station ξ_F. We first rewrite Eq. (3) with explicit dependence of ξ_F on p as

$$\xi_{n+1} - \xi_F(p) \simeq \mathbf{M}[\xi_n - \xi_F(p)] , \tag{5}$$

where $\xi_F(p_n) \simeq \xi_F(0) + \mathbf{g}p_n$ in a linear approximation (this relation being the operational definition of $\mathbf{g}$). Notice that $\mathbf{M}$ is assumed to be p independent, in agreement with Ref. [4]. Once the trajectory enters the control station [ball $B_\epsilon(\xi_F)$], we seek the value p_n that minimizes the norm $\|\hat{\xi}_{n+1}(p_n) - \xi_F(0)\|$, where $\hat{\xi}_{n+1}(p_n)$ is the prediction for ξ_{n+1} obtained from Eq. (5) taken as a strict equality. This expresses the condition that the next expected return on the Poincaré section, after application of perturbation p_n, must lie in a neighborhood close to the fixed point:

$$\begin{aligned} \|\hat{\xi}_{n+1}(p_n) - \xi_F(0)\| &= \|p_n(\mathbf{g} - \mathbf{M}\mathbf{g}) + \mathbf{M}[\xi_n - \xi_F(0)]\| \\ &= \text{minimum} . \end{aligned} \tag{6}$$

We set $\boldsymbol{\alpha} \equiv \mathbf{g} - \mathbf{M}\mathbf{g}$ and $\boldsymbol{\beta} \equiv \mathbf{M}[\xi_n - \xi_F(0)]$. This yields

$$p_n = p_{\min} \equiv -\frac{\boldsymbol{\alpha}\cdot\boldsymbol{\beta}}{\|\boldsymbol{\alpha}\|^2} = -\frac{(\mathbf{g} - \mathbf{M}\mathbf{g})\cdot\{\mathbf{M}[\xi_n - \xi_F(0)]\}}{\|\mathbf{g} - \mathbf{M}\mathbf{g}\|^2} . \tag{7}$$

The optimal (minimal) distance achievable is hence $\|-(\hat{\boldsymbol{\alpha}}\cdot\boldsymbol{\beta})\hat{\boldsymbol{\alpha}} + \boldsymbol{\beta}\|$, where $\hat{\boldsymbol{\alpha}} \equiv \boldsymbol{\alpha}/\|\boldsymbol{\alpha}\|$. Notice that if ξ_n is already close to the stable manifold of $\xi_F(0)$, its predicted image $\hat{\xi}_{n+1}(p_n)$ will be close to the target point $\xi_F(0)$, so that Eq. (7) will yield a small correction p_n, in agreement with the OGY algorithm. We also define a range for the control parameter, $-p_* < p < p_*$, so that no control is attempted if the computed p overshoots these limits.

This procedure does not require us to determine the stability properties of the orbit and allows us to fit the

Poincaré map with a generic polynomial function, rather than with a simple linear application, thus leading to improved predictions. Moreover, depending on the computing time restrictions, it is possible to complement it with noise-reduction algorithms. In particular, the vector **g** should be estimated as an average over subsequent displacements $\xi_F(p_n)-\xi_F(0)$, for $n=1,2,\ldots$, in order to improve the initial guess (which, as mentioned above, represents a major source of inaccuracy). The method may also be modified according to the suggestions of Ref. [16], so that the value p_n of the perturbation at time n is made dependent on its previous values as well. A practical implementation of this criterion, however, has proved to be rather problematic.

IV. RESULTS

Periodic orbits of order up to 6 have been located online with relative error $d(\mathbf{x}_i,\mathbf{x}_{i+n})/\epsilon_i \approx 10^{-2}$ under various experimental conditions. Good agreement has been found with the corresponding orbits computed from a suitable differential model [1]. An independent verification of the method has been obtained by analyzing the NMR laser with a delay line. In such a case, the periods are no longer exact multiples of a fundamental one. The experiment has been performed a large number of times in the region delimited by a circle in Fig. 1, where the (ω, A) parameter space is reported. The numbers indicate regions with stable periodic behavior of the corresponding order (2 and 2* are two different period-2 trajectories). A few of the lowest-order orbits for the Q-modulated laser are displayed in Fig. 2. The control station ξ_F can be set interactively anywhere on the target γ, which is itself chosen out of a number of closely returning orbits.

The statistical reliability of the estimated matrix **M**

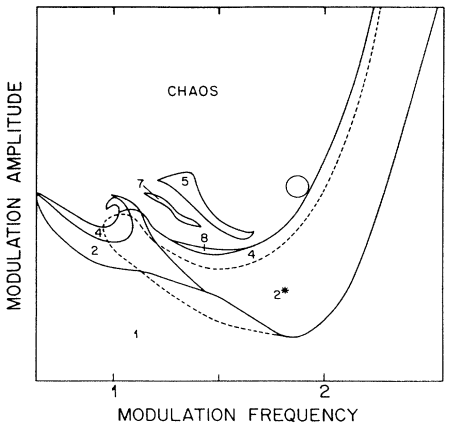

FIG. 1. Parameter space (ω, A) for the NMR laser, representing the regions of stable periodic and chaotic behavior in dependence on the frequency ω and amplitude A of the modulation. Arbitrary units have been used for the A axis, while the frequency has been rescaled to the resonant one. The numbers indicate the order of the periods. The symbols 2 and 2* correspond to two different period-2 orbits. The circle encloses the domain in which control has been performed.

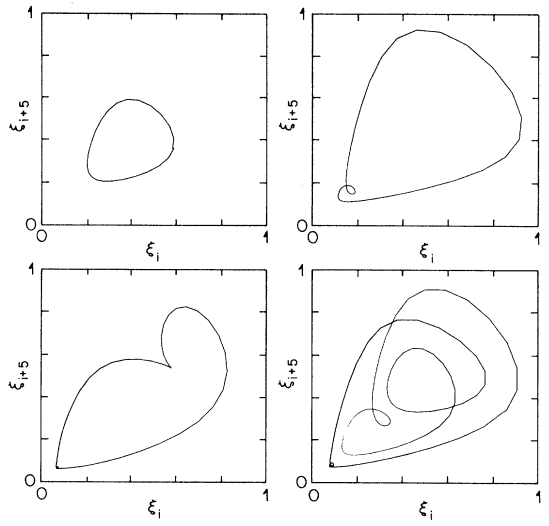

FIG. 2. Two-dimensional projections of unstable periodic orbits for the NMR laser, previously located in a six-dimensional embedding space. The periods 1, 2, 3, and one of the periods 5 are shown.

sensibly depends on the position on γ, on the ball radius ϵ, and on the number m of fit points. The typical χ^2 values, rescaled to ϵ^2, were in the range $(10^{-3}, 10^{-1})$, except in the most crowded regions of the attractors (where the dynamics is most affected by the noise) which have not been selected for control. The corresponding ϵ values, for $a \in (0.3, 0.6)$ lay in the interval (50,300) for $E=6$ (recall that the data are 12-bit integers, i.e.,

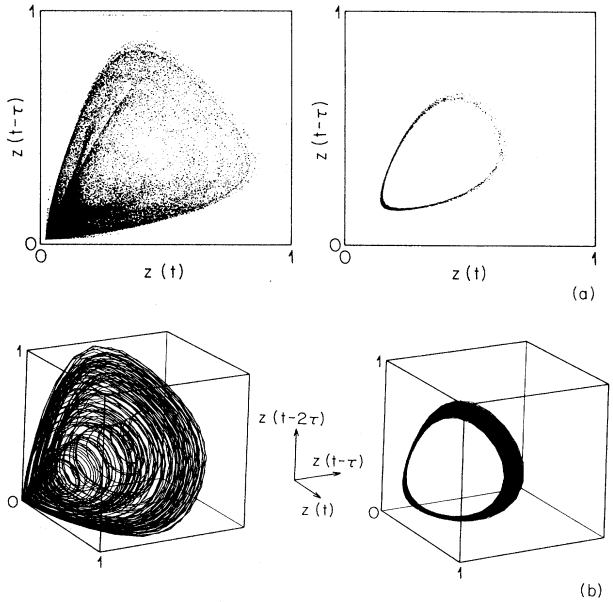

FIG. 3. Two- and three-dimensional projections [(a) and (b), respectively] of the chaotic attractor (left) and of the period-1 orbit controlled with OGY's method (right). The figure corresponds to a measurement of about 5 s. The control persisted for over one hour.

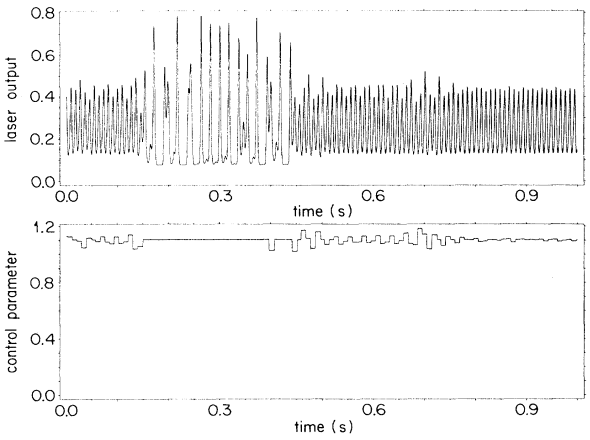

FIG. 4. Time evolution of the laser output (upper trace) and of the control signal (lower trace) during the stabilization of the period-1 orbit with the OGY method. A short outburst is visible. The algorithm was able to recover the control successfully.

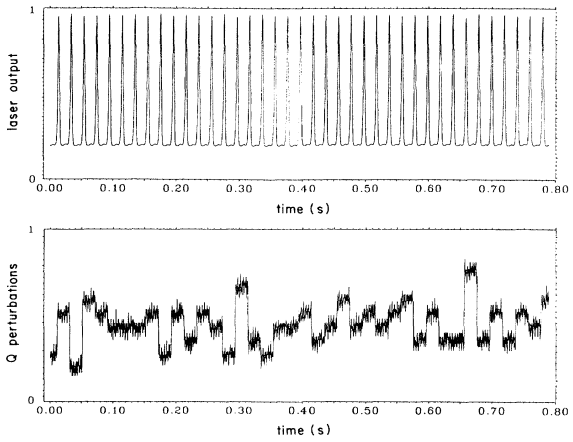

FIG. 5. Same as in Fig. 4 for a period-2 orbit, stabilized with the minimal expected deviation (MED) method. No spontaneous outburst has been observed for over two hours of laser activity. Notice the smallness of the control-signal amplitude, in comparison with that of Fig. 4.

$z \in [0,4096]$). The fits have been usually carried out with sets of $m = 50-100$ nearest neighbors.

In Fig. 3, we present two- and three-dimensional projections of the chaotic attractor and of the period-1 orbit controlled with OGY's method, for a time length of 5 s. In Fig. 4 we show the laser output and the control signal for a short time interval during the same experimental run. Although an outburst is clearly visible in this plot, the system was indeed stable for over one hour and the method has been able to recover the target motion after several external disturbances (including shooting of champagne corks). The length of the outbursts never exceeded half a second. The maximal perturbation $p_{\max}$, relative to the amplitude A of the modulation, was $p_{\max}/A \approx 0.07$. The stabilization of higher-order orbits, however, was much more difficult because of the above-mentioned problems: a single control station on the curve γ was often not sufficient and complex eigenvalues occurred whenever more control stations have been considered. Only periods 2 and 4 have been occasionally controlled. The difficulties arise from the speed of the system, the presence of noise, and the statistical uncertainty of the matrix evaluations which affect, especially, the components of the vector $\mathbf{f}_u$. On the other hand, the accuracy of the predictions, directly performed with the matrix $\mathbf{M}$, turned out to be considerably more reliable.

The minimal expected deviation technique, being based on the matrix $\mathbf{M}$ rather than on $\mathbf{f}_u$, proved to be more efficient. For example, the period-2 orbit has been stabilized in a highly reproducible way by applying a much smaller relative perturbation ($p_{\max}/A \leq 0.02$). The recovery time upon external disturbances was also appreciably shorter. No spontaneous outbursts have been observed for times of the order of two hours or more. This technique appears to be less sensitive to noise. The maximal deviation from the target remained below the value $d_{\max} \approx 300$ in six dimensions. The output and control signals are displayed in Fig. 5, to be compared with Fig. 4. The largest eigenvalue of the period-1 orbit is $\lambda_u^{(1)} = -2.0 \pm 0.1$, whereas that of the period-2 orbit is $\lambda_u^{(2)} = -1.3 \pm 0.1$. The latter orbit, however, passes very close to the origin, where the signal-to-noise ratio is small, and is therefore much harder to control.

V. CONCLUSIONS

We achieved a full implementation of the OGY control method in a chaotic NMR laser working at frequencies of the order of 120 Hz in a six-dimensional embedding space. To this end, we identified all unstable periodic orbits up to order 6 and evaluated their stability properties. The quality of the control, i.e., average distance from the target and frequency of the outbursts, strongly depends on the estimated quantities $\mathbf{M}$, $\mathbf{f}_u$, and $\mathbf{g}$. The minimal expected deviation method simplifies the analysis, in that it does not require explicit calculation of $\mathbf{f}_u$.

Unstable orbits with high period need a larger number of control stations for the control to be successful. A common problem encountered in such cases is the occurrence of multiple unstable and complex eigenvalues in the linearized dynamics. This drawback is not shared by the minimal expected deviation method which proved to be more robust than OGY's.

ACKNOWLEDGMENTS

We acknowledge very constructive collaboration with M. Finardi and J. Simonet and partial support by the Swiss National Science Foundation.

[1] L. Flepp, R. Holzner, E. Brun, M. Finardi, and R. Badii, Phys. Rev. Lett. **67**, 2244 (1991).
[2] J. D. Farmer and J. J. Sidorowich, in *Evolution, Learning and Cognition,* edited by Y. C. Lee (World Scientific, Singapore, 1988), pp. 277–330.
[3] E. J. Kostelich and J. A. Yorke, Phys. Rev. A **38**, 1649 (1988).
[4] E. Ott, C. Grebogi, and J. A. Yorke, Phys. Rev. Lett. **64**, 1196 (1990).
[5] E. Ott, C. Grebogi, and J. A. Yorke, in *Chaos: Soviet-American Perspectives on Nonlinear Science,* edited by D. K. Campbell (AIP, New York, 1990), pp. 153–172.
[6] W. L. Ditto, S. N. Rauseo, and M. L. Spano, Phys. Rev. Lett. **65**, 3211 (1990).
[7] R. Roy, T. W. Murphy, Jr., T. D. Maier, and Z. Gills, Phys. Rev. Lett. **68**, 1259 (1992).
[8] J. Singer, Y.-Z. Wang, and H. H. Bau, Phys. Rev. Lett. **66**, 1123 (1991).
[9] A. Azevedo and S. M. Rezende, Phys. Rev. Lett. **66**, 1342 (1991).
[10] R. Henn, F. Rödelsperger, and H. Benner, in *Proceedings of the 26th Congress Ampere on Magnetic Resonance,* edited by A. Anagnostopoulos *et al.* (NCSR "Demokritos", Athens, 1992).
[11] A. Hübler and E. Lüscher, Z. Naturwiss. **76**, 67 (1989); E. A. Jackson, Physica D **44**, 407 (1990).
[12] E. Brun, B. Derighetti, D. Meier, R. Holzner, and M. Ravani, J. Opt. Soc. Am. B **2**, 156 (1985).
[13] C. Broggi, Ph.D. thesis, University of Zurich, 1988.
[14] F. Takens, in *Dynamical Systems and Turbulence,* edited by D. Rand and L. S. Young (Springer-Verlag, Berlin, 1981), p. 230.
[15] W. H. Press *et al.*, *Numerical Recipes* (Cambridge University Press, Cambridge, England, 1986).
[16] U. Dressler and G. Nitsche, Phys. Rev. Lett. **68**, 1 (1992).